Cai *et al. Cancer Cell International* (2024) 24:215
https://doi.org/10.1186/s12935-024-03351-z

Cancer Cell International

RESEARCH Open Access

CDK4/6 inhibition enhances T-cell immunotherapy on hepatocellular carcinoma cells by rejuvenating immunogenicity

Xiurong Cai[1,2†], Guo Yin[3†], Shuai Chen[4], Frank Tacke[3], Adrien Guillot[3] and Hanyang Liu[3,4*]

Abstract

Hepatocellular carcinoma (HCC) poses a significant clinical challenge, necessitating the integration of immunotherapeutic approaches. Palbociclib, a selective CDK4/6 inhibitor, has demonstrated promising efficacy in preclinical HCC models and is being evaluated as a novel therapeutic option in clinical trials. Additionally, CDK4/6 inhibition induces cellular senescence, potentially influencing the tumor microenvironment and immunogenicity of cancer cells. In this study, we conducted comprehensive bioinformatic analyses using diverse HCC transcriptome datasets, including bulk and single-cell RNA-sequencing data from public databases. We also utilized human and mouse HCC cells to investigate functional aspects. Primary T cells isolated from mouse blood were employed to assess T cell immunity against HCC cells. Results revealed that $CD8^+$ T-cell infiltration correlates with improved outcomes in HCC patients with suppressed CDK4/6 expression. Moreover, CDK4/6 expression was associated with alterations in the immune landscape and immune checkpoint expression within the liver tumor microenvironment. Furthermore, we found that treatment with Palbociclib and Doxorubicin induces cellular senescence and a senescence-associated secretory phenotype in HCC cells. Notably, pretreatment with Palbociclib augmented T cell-mediated cytotoxicity against HCC cells, despite upregulation of PD-L1, surpassing the effects of Doxorubicin pretreatment. In conclusion, our study elucidates a novel mechanism by which CDK4/6 inhibition enhances T-cell-associated cancer elimination and proposes a potential therapeutic strategy to enhance T-cell immunotherapy on HCC.

Introduction

Hepatocellular carcinoma (HCC) stands as a leading cause of cancer-related mortality on a global scale [1]. The HCC incidence is attributed to diverse risk factors, including chronic viral hepatitis, fatty liver disease, alcohol-related liver cirrhosis, smoking, obesity, diabetes, iron overload, and various dietary exposures, all of which lead to hepatic injury, cirrhotic progression, and inflammation, causing hepatic carcinogenesis [2]. Conventional therapy modalities for HCC include surgical resection, liver transplantation, percutaneous ablation, and transarterial chemoembolization, and systemic chemotherapy

†Xiurong Cai and Guo Yin contributed equally to this work.

*Correspondence:
Hanyang Liu
hanyang.liu@charite.de

Full list of author information is available at the end of the article

Graphical abstract

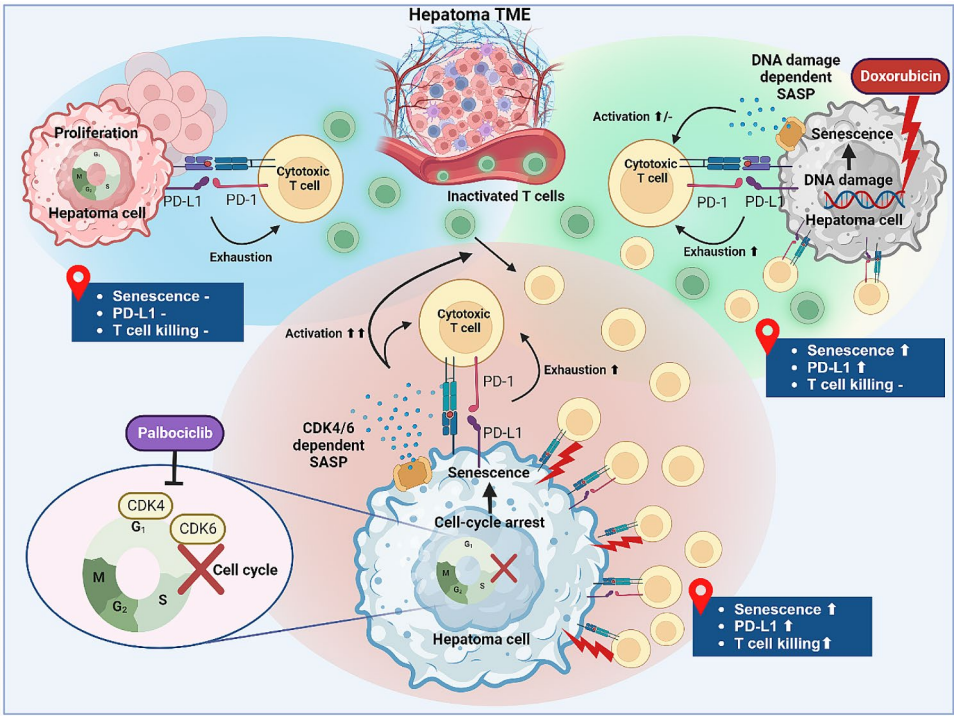

Keywords Cell-cycle arrest, Immunostimulation, Hepatoma, Palbociclib, Doxorubicin, Immunotherapy

[3]. In the past decade, immunotherapies, especially immune checkpoint inhibitors (ICIs) have emerged to bring the clinical management of advanced HCC to the next level. However, poor immune infiltration and dysregulated immunogenicity of cancer cells contribute to persistent immune suppression in solid tumors including HCC (known as 'cold tumor'), leading to a steep rise in treatment failures [4]. Enhancing the immunogenicity of cancer cells and activating specific cytotoxic T cells are key factors for improving therapeutic efficacy against cancer.

Uncontrolled proliferation of cancer cells can be disrupted by cell cycle interference, which is indicated as a powerful treatment target for anti-cancer therapy. Accordingly, several selective inhibitors targeting cyclin-dependent kinase 4/6 (CDK4/6) have been applied to cancer treatment [5, 6]. Furthermore, cellular senescence, one of the steady cell-cycle arresting programs, mediates a dynamic state of cell fate transition. In malignant lesions, senescence and programmed cell death (PCD) can terminate the successive expansion of cancer cells intrinsically through cell cycle arrest [7]. Nonetheless, unlike PCD, senescent cancer cells may restore immunogenicity not only through the senescence-associated secretory phenotype (SASP) but also by upregulating interferon γ-sensing and antigen-processing mechanisms to trigger adaptive T-cell surveillance [8, 9]. Last but not least, immune checkpoints (e.g., PD-L1) were found enriched in senescent liver cancer cells, mediating a suppressive tumor microenvironment and T-cell exhaustion, which can be partially reversed by immune checkpoint blockade [9–12]. The complex role of senescence in anti-HCC treatment, especially in immunotherapies requires further investigation.

Here, we provide an explorative study to depict the comprehensive anti-cancer functions of CDK4/6 inhibition in HCC. According to the patient-derived liver cancer genomic data cohort, CDK4 and CDK6 were defined as key cell cycle regulators in HCC with high relevance to T-cell cytotoxicity and clinical outcomes. Interestingly, transcriptome analysis and in vitro investigations of CDK4/6 inhibition on HCC cells (HCs) revealed that CDK4/6-dependent cellular senescence broadly altered the levels of inflammatory factors and immune checkpoints in cancer cells. Taken together, our study elucidates a novel mechanism that CDK4/6 inhibition antagonizes senescence-related T-cell exhaustion via revitalizing immunogenicity in HCC.

Methods and materials

Data source and analysis

Transcriptome datasets of liver cancers were obtained from the Cancer Genome Atlas Program (TCGA) and Gene Expression Omnibus (GEO) database (supplementary Table 1). Differentially expressed genes (DEGs) between groups were sorted out by limma package [13] with log (fold change, FC) > 1.5 and $p < 0.05$. Pathological immunohistochemistry images from liver tumor and non-tumor tissue samples were obtained from Human Protein Atlas (HPA) database.

Gene profiling in liver hepatic carcinoma (LIHC)

The Gene Expression Profiling Interactive Analysis (GEPIA) [14] was applied to investigate LIHC and normal liver tissue respectively based on gene profiling of TCGA [15] and the Genotype-Tissue Expression (GTEx) [16]. We analyzed the expression levels of candidate genes in relation to overall survival (OS), disease-specific survival (DSS), progression-free survival (PFS), and disease-free survival (DFS). Survival time was analyzed and displayed using the Kaplan–Meier plotter. The mean follow-up time was above 10 years, and the Cox p-value was analyzed. The gene mutation landscape was analyzed to reveal related oncogene mutation by the ComplexHeatmap R package and plotted by the oncoprint [17].

Enrichment analysis and immune composition prediction

Function enrichment analysis was performed based on Gene ontology (GO) [18] and the Kyoto Encyclopedia of Genes and Genomes (KEGG) databases [19]. The Tumor Immune Estimation Resource (TIMER) database was introduced to assess the main immune cell infiltration and related cancer outcome, based on the TCGA database [20]. Cell composition of complex tissues from their gene expression profiles was characterized by the CIBERSORT method [21].

Single-cell transcriptome analysis

Single-cell transcriptome dataset was obtained from the GEO database (supplementary Table 1). R packages (Seruat [22], CellChat [23], and ggplot2 [24]) were utilized to depict cell types, gene expression, and cell interactions.

Cell culture

The human and murine HCC cell lines (HepG2 and Hepa1-6) were cultured in the complete medium [10% FBS + 90% DMEM medium-high glucose mixed with 1% penicillin-streptomycin (100 Units/mL)]. Primary murine T cells were cultured in the RPMI 1640 medium supplemented with 10% FBS + 1% penicillin-streptomycin + 2 mM L-Glutamine + 1% non-essential amino acids + 1% pyruvate solution. All the cells were maintained in a humid incubator at 37℃ with 5% CO_2.

Multiplex enzyme-linked immunosorbent assay (ELISA) detection

Supernatant samples were collected from cell culture at the end point of experiments. Concentrations of IFNγ, IL-1β, IL-6, and TNFα were detected using a Mouse Cytokine Panel 2 (4-Plex) purchased from Beijing Biolink Biotechnology Co.,Ltd (Beijing, China). The detection was performed following the manufacturer's instructions. Fluorescence reading was acquired using a microplate reader (Thermo Fisher, USA).

Cell viability measurement

HepG2 and Hepa1-6 cells were seeded in 96-well plates (5000 / well). CCK-8 solution was added to each well at the end point of experiments (10 μl / 100 μL medium). Fluorescence reading was acquired using a microplate reader (Thermo Fisher, USA) after 2-hour incubation at 37℃ with 5% CO_2. The CCK-8 kit was purchased from Beyotime Biotechnology (Shanghai, China).

Senescence induction and detection

The HCC cells were treated with either Palbociclib or Doxorubicin in a concentration gradient for five days. The senescence-associated beta-galactosidase (SA-β-Gal) staining was performed according to the manufacturer's instructions. The SA-β-Gal^+ cells were imaged under a microscope (Olympus, Japan) and quantified using Fiji software (NIH Image, USA). The treatment-containing medium was replaced by a fresh complete medium once senescence was induced.

T-cell isolation and stimulation

C57BJ/6 mice were obtained from the animal core facility of Nanjing Medical University (Jiangsu, China). Animal experiments were approved by the Animal Welfare Committee of the affiliated Changzhou Second People's Hospital of Nanjing Medical University [Approval No. (2020) KYO 045 − 05]. Mouse spleens were harvested and dissociated using a gentleMACS dissociator. The single-cell suspension was then filtered through a 40 μm mesh filter to remove possible cell clumps and centrifuged at 1,500 rpm for 5 min (4℃). The pellet was incubated with red cell lysis buffer for 10 min at room temperature. Then, the cell suspension was washed twice with pre-chilled 1× PBS and proceeded to pan-T cell isolation according to the manufacturer's instruction (Miltenyi, USA). The untouched T cells were stimulated with detachable CD3/CD28 Dynabeads™ in the complete T-cell medium supplemented with murine IL-2 (30 Units/mL) for 3 days according to the manufacturer's instructions of Dynabeads.

T-cell cytotoxicity assay and live-cell imaging

Pre-activated murine primary T cells were introduced and co-cultured with senescent HCC cells at a certain ratio (T-cell: HCC=5:1). The T-cell cytotoxicity assays were determined by labeling damaged HCC cells using propidium iodide (PI) dye, which was monitored under the microscope (Olympus, Japan) for 72 h and assessed at the end point using a fluorescent microscope (Olympus, Japan). Protein levels of Ki67, γ-H2AX, and PD-L1 were detected using the immunocytochemistry protocol based on paraformaldehyde-fixed cells. Images were obtained under a fluorescent microscope (Olympus, Japan) and analyzed using Fiji software (NIH Image, USA). Antibodies and fluorescent dyes used in this study are listed in supplementary Table 2.

Flow cytometry

Mouse primary T cells were collected and centrifuged at 1,500 rpm for 5 min, followed by washing twice with 1× PBS. Then, cell samples were sequentially stained with a viability dye (Ghost Dye™ Violet) and primary conjugated antibodies according to the manufacturer's instructions. Data was obtained using a spectral flow cytometer (Canto II, BD, USA), and analyzed using FlowJo software 10.9 (BD, USA). Antibodies and fluorescent dyes used in this study are listed in supplementary Table 2.

Cellular calcium detection

Mouse primary T cells were seeded in 96-well plates. After the corresponding treatments, intracellular calcium was incubated following the instructions of the Fluo-4 NW Calcium Assay Kit (Thermo Fisher, USA). Simultaneously, cells were incubated with the Calmodulin-1/2/3 antibody after paraformaldehyde fixation. Fluorescence reading was acquired using a microplate reader (Thermo Fisher, USA). Cell numbers were estimated using a flow cytometer (Canto II, BD, USA). Fluorescence readings were normalized by the estimated live cell number of each group.

Gene expression quantification

Total RNA was extracted from cell homogenate using TRIzol® reagent (Invitrogen; Thermo Fisher Scientific, Waltham, MA, USA). Reverse transcription was conducted with a PrimeScript™ RT Reagent Kit (Takara Biotechnology Co., Ltd., Tokyo, Japan), and real-time quantification was subsequently performed using a SYBR® Premix Ex Taq Kit (Takara Biotechnology Co., Tokyo, Japan). The relative RNA expression levels were calculated using the -ΔΔCt method. Mouse primers included in this study are listed in supplementary Table 3.

Statistical analysis

GraphPad Prism 10.0 software (GraphPad Software, Inc., USA) and RStudio (Posit, USA) were used to generate plots. Significant differences were identified using an unpaired t-test. Pearson correlation analysis was performed to calculate the correlation coefficients. "$p<0.05$" commonly indicates a statistically significant difference.

Results

CDK4/6 expression correlates with immune infiltration and outcomes of liver cancer

LIHC datasets were obtained from the TCGA database. Functional enrichment analyses (GO and KEGG) were conducted with upregulated DEGs (tumor vs. non-tumor), showing that the cell cycle process was the most significantly enriched biological process (Fig. 1A and B). Among all the CDKs, *CDK1* and *CDK4* were drastically overexpressed (tumor vs. non-tumor) (Fig. 1C). The OS and RFS of LIHC patients were correlated with low expression of CDK1, 2 and 4 (Fig. 1D). Hence, expression of *CDK1*, *CDK2*, and *CDK4* demonstrated a significantly positive correlation with liver cancer stages (Fig. 1E and Supplementary Fig. 1A). In addition, we retrieved several published bulk RNA-sequencing datasets related to human HCC livers (GSE146719, GSE169289, GSE184733, GSE105130 and GSE166163). *CDK4* expression was found significantly upregulated in tumor lesions from all datasets (Fig. 1F). Correlation of immune cell infiltration and CDKs (*CDK1*, *CDK2*, *CDK4*, and *CDK6*) was assessed from TCGA-LIHC and HCC datasets, which showed complex and contradictory results (Supplementary Fig. 1B and C). Protein-protein interactions between CDKs and immune checkpoints were also investigated and disclosed (Supplementary Fig. 1D). The interaction of *CDK4/6* expression and immune cell infiltration [dendritic cells (DC), M0 / M1 /M2 macrophages and $CD4^+$/$CD8^+$ T cells] in influencing the disease outcome of HCC patients was assessed, which showed that $CD8^+$ T-cell infiltration with low CDK6 expression predicted the significant improvement of disease outcome (Fig. 1G and Supplementary Fig. 1E). In situ protein measurement based on immunohistochemistry (IHC) was obtained from HPA database. It showed that CDK4 and CDK6 protein levels increased in parenchymal areas (tumor vs. non-tumor) (Fig. 1H), while CDK1 and CDK2 remained undetectable (data not shown). Taken together, the cell-cycle regulators CDKs (especially CDK4) play crucial roles in the disease prognosis of HCC.

Palbociclib and Doxorubicin enhance senescence and PD-L1 levels on HCs

To reveal the functions of CDK4/6 inhibition and DNA damage on HCs, Palbociclib (Palb) and Dox were introduced. Concentration-dependent cytotoxicity of Palb

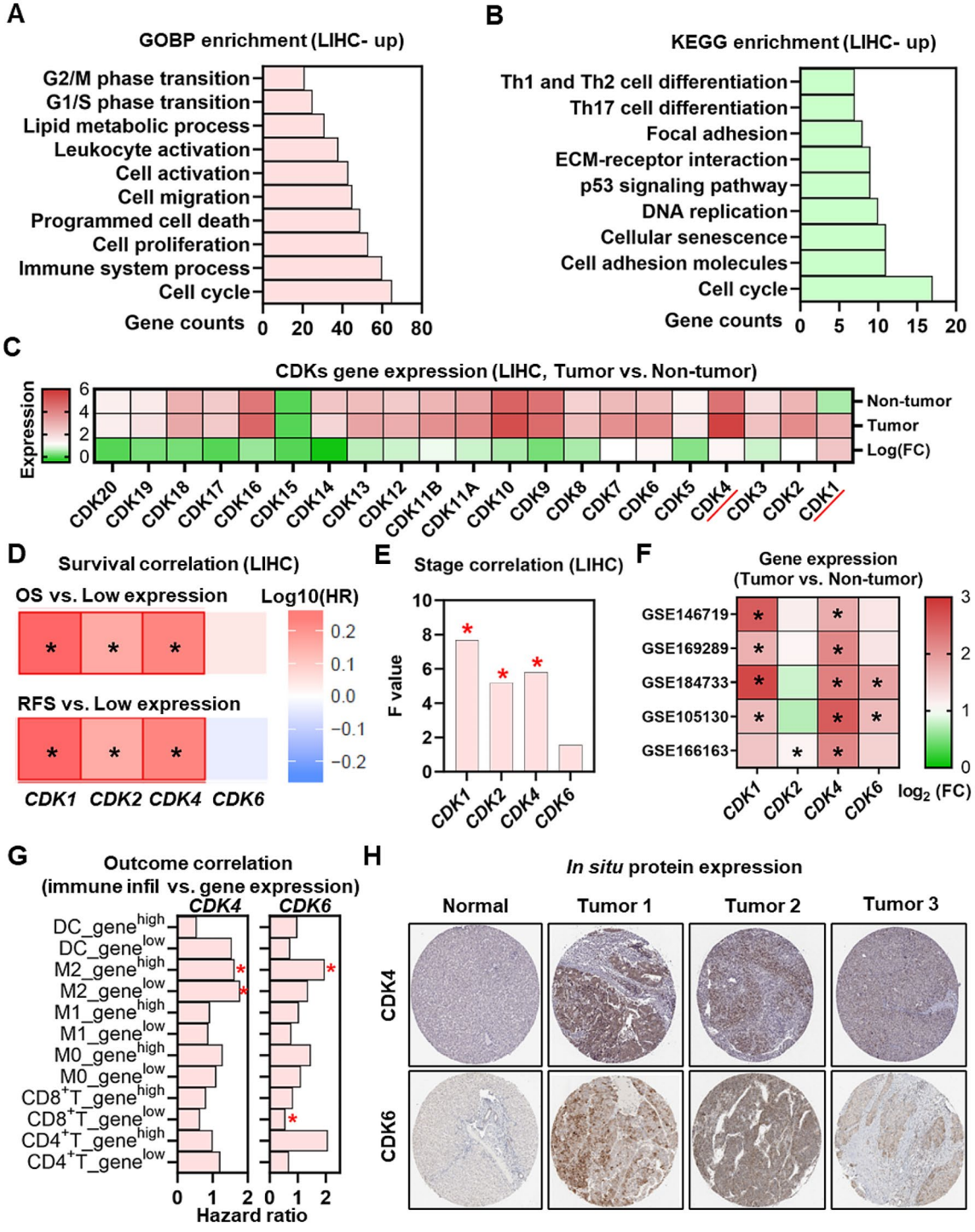

Fig. 1 CDKs characterized by bulk transcriptome analysis from HCC patient cohorts. (**A**) GO and (**B**) KEGG enrichment analyses based on significantly upregulated genes (LIHC, Tumor vs. Non-tumor) were displayed. (**C**) Gene expression of CDKs in non-tumor and tumor samples, as well as fold changes, was displayed. (**D**) Correlation between CDKs (*CDK1*, *CDK2*, *CDK4*, and *CDK6*) and survival time (OS and RFS) was displayed. (**E**) Correlation between CDKs (*CDK1*, *CDK2*, *CDK4* and *CDK6*) and liver cancer stages was displayed. (**F**) Expression of *CDK1*, *CDK2*, *CDK4*, and *CDK6* was demonstrated based on five liver cancer databases. (**G**) HCC outcome correlating with expression of CDK4/6 and immune cell infiltration was illustrated. (**H**) In situ expressions of CDK4 and CDK6 were depicted on liver tumor and non-tumor tissue samples. "*" represents $p < 0.05$

and Dox was titrated on human (HepG2) and mouse (Hepa1-6) HCC cell lines to select suitable concentrations (6 μM of Palb and 50 ng/mL of Dox) (supplementary Fig. 2A-D). Palb and Dox drastically suppressed proliferation of HepG2 and Hepa1-6 cells within 6 days, while Palb maintained cell numbers of Hepa1-6 from day 3 to day 6 (Fig. 2A and B). Simultaneously, cellular senescence induction by Palb and Dox was titrated on both cell lines, which suggested that Hepa1-6 responded better upon senescence induction (Supplementary Fig. 3A and 3B). Upon Palb or Dox treatment, cellular proliferation in Hepa1-6 was assessed through Ki67 staining (Fig. 2C) and the calculation of proliferation ratios (Fig. 2D), which showed that both Palb and Dox can drastically suppress HC proliferation. Furthermore, cellular senescence was detected by the accumulation of cytoplasmic SA-β-GAL (Fig. 2E, quantification is displayed in Fig. 2F) and nuclear γ-H2AX (Fig. 2G, quantification is displayed in Fig. 2H), the results of which showed that both Palb and Dox can significantly induce HC senescence. In addition, PD-L1 expression was upregulated on HCC cells after treatment with either Palb or Dox (Fig. 2I, quantification is displayed in Fig. 2J). Taken together, Palb and Dox were evidenced to induce cellular senescence and inflammatory cytokine production in HCs.

CDK4/6 suppression exaggerates HCC immunogenicity by altering inflammatory secretion

Interactive diversity among HCC cells and immune cells was depicted using a single-cell transcriptome HCC dataset. Cell types [HCC, hepatic stellate cell (HSC), endothelial cell, B cell, T cell and myeloid cell] were clustered and displayed with UMAP (Fig. 3A). Samples from 2 HCC patients were classified (Fig. 3B). The expressions of *CDK4* and *CDK6* were illustrated, characterizing HCC sample 1 as $CDK6^{low}$ and sample 2 as $CDK6^{high}$ (Fig. 3C). Furthermore, the abundance of extracellular signaling interactions was displayed (Supplementary Fig. 4A). $CDK6^{low}$ HCC cells transmit more biological signals (e.g., cytokines, ligands) to T cells in contrast to $CDK6^{high}$ HCC cells (Fig. 3D, full interaction profile in Supplementary Fig. 4B). Inflammatory signaling interactions were assessed among HCs, T cells and myeloid cells, illustrating a richer abundance of T-cell response trigger-proteins, including IL2, LT, LIGHT, TGF-β, BLTA, CD80, VCAM, ICAM and ITGB2 signals, in $CDK6^{low}$ samples compared to $CDK6^{high}$ samples (Fig. 3E, full interaction profile in Supplementary Fig. 4C). These results implied that HCC cells with low *CDK6* expression can potentially activate T-cell immune response. In addition, transcriptome datasets were obtained from CDK4/6-suppressed (GSE145389) and Doxorubicin (Dox)-administrated (GSE145389) human HCC cell lines. KEGG functional enrichment analysis was conducted with the significantly upregulated DEGs (siCDK4/6 vs. siCtrl and Dox vs. Vehicle). CDK4/6 inhibition induced broader alterations in signals regulating cell fates, metabolism, and inflammation (Fig. 4A), while Dox-treatment mainly triggered cell damage and cell-cell interactions (Fig. 4B). Additionally, investigations of common inflammatory secretome revealed that the abundance of inflammatory cytokines was more augmented by CDK4/6 inhibition than Dox-treatment (Fig. 4C and D). Simultaneously, typical immune checkpoints (*CD274*, *CD276*, *CD80*, *HLA-A*, *HLA-G* and *GALNT9*) were checked. Interestingly, *CD274* expression was downregulated upon CDK4/6 inhibition, but upregulated upon Dox-treatment (Fig. 4E and F). Furthermore, gene expression of inflammatory cytokines and immune checkpoints was measured in HepG2 and Hepa1-6 cells. In HepG2, Palb significantly upregulated the expression of *IL1B* and *TNFA* but downregulated the expression of *IL7*. Dox significantly upregulated the expression of *IL6*, *IL10*, *IL15*, *IFNG* and *CD80*, but downregulated the expression of *CD274*. In Hepa1-6, Palb significantly upregulated the expression of *Il1a*, *Il1b*, *Il6*, *Il15*, *Il23*, *Ifng*, *Tnfa* and *Cd274*, but downregulated. Dox significantly upregulated the expression of *Il6* and *Il13* but downregulated the expression of *Il12* and *Il15* (Fig. 4G). Palb drastically enhanced secretion of IL1β, IL6 and IFNγ in Hepa1-6 cells, while Dox drastically enhanced the secretion of IL6 and IFNγ (Fig. 4H). Taken together, CDK4/6 inhibition can regulate the immunogenicity of HCC cells, particularly via altering inflammatory secretion.

CDK4/6 inhibition-dependent HC senescence revitalizes T-cell cytotoxicity

To understand the efficacy of immunotherapies targeting senescent HCs, PD-1 or PD-L1 blockade combined with primary splenic T cells from strain-matched wild-type mice was introduced and co-cultured with either Palb- or Dox-induced senescent Hepa1-6 cells. T-cell-mediated cytotoxicity against HCC cells was tracked and monitored for 96 h (Fig. 5A). After administration of HC-derived conditioned medium (CM), T cells were characterized by flow cytometry (Supplementary Fig. 6). The proportion of $CD4^+$ T cells in total T-cell population increased significantly only after treatment with Dox-CM compared to vehicle CM, while $CD8^+$ T-cell proportion decreased significantly after treatment with Dox-CM (vs. Palb-CM and vs. vehicle CM) (Fig. 5B). $CD69^+$ cell proportions conventionally declined in T cells receiving CM treatment compared to the ex vivo expanded T cells as a positive control (Fig. 5C and D). $CD69^+$ $CD4^+$ T-cell proportion significantly increased in T cells treated with either Palb-CM or Dox-CM compared to vehicle CM (Fig. 5C), whereas $CD69^+$ $CD8^+$ T-cell proportion remained comparable in T cells receiving either Palb-CM

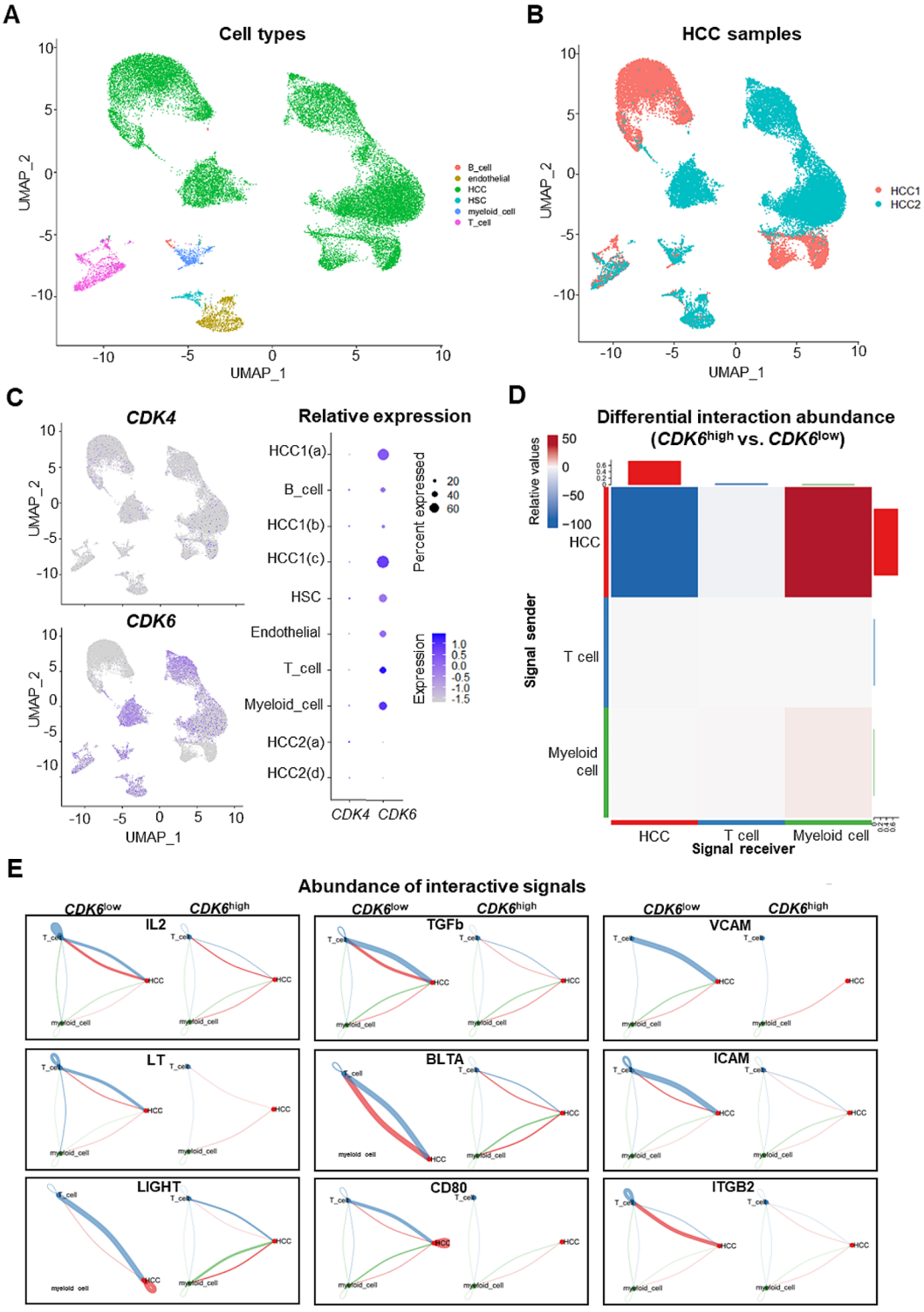

Fig. 2 Single-cell transcriptome analysis depicting CDK4/6 expression and immune interactions in human HCC samples. (**A**) Cell types (HCC, HSC, endothelial cell, B cell, T cell, and myeloid cell) and (**B**) HCC samples were clustered with UMAP. (**C**) Expression of *CDK4* and *CDK6* was illustrated. (**D**) The abundance of outgoing and incoming signals from variable cell populations was displayed. (**E**) Inflammatory signaling interactions were assessed among HCs, T cells, and myeloid cells. The thickness of the arrows represents interaction abundance

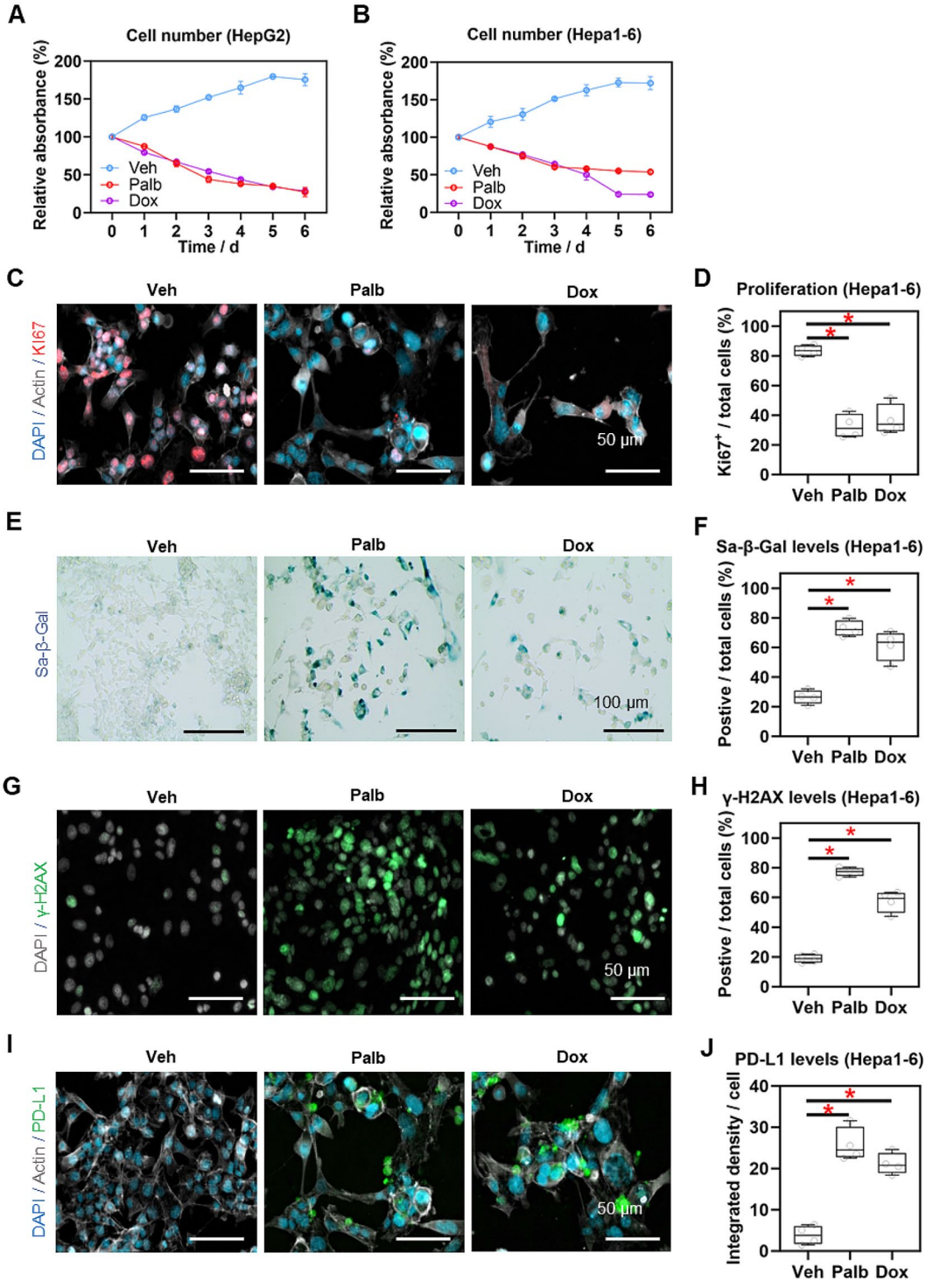

Fig. 3 Cellular senescence and PD-L1 upregulation on HCC cells induced by Palbociclib and Doxorubicin. Cellular proliferation ($Ki67^+$) of Hepa1-6 cells under Vehicle, Palbociclib- and Doxorubicin-treatment was displayed (**C**) and quantified (**D**). SA-β-GAL (**E**) and γ-H2AX (**G**) levels of Hepa1-6 cells under Vehicle, Palbociclib- and Doxorubicin-treatment were displayed and quantified **(F & H)**. PD-L1 level of Hepa1-6 cells under Vehicle, Palbociclib- and Doxorubicin-treatment was displayed **(I)** and quantified **(J)**. Abbreviation: Veh: Vehicle, Palb: Palbociclib, Dox: Doxorubicin. "*" represents $p < 0.05$

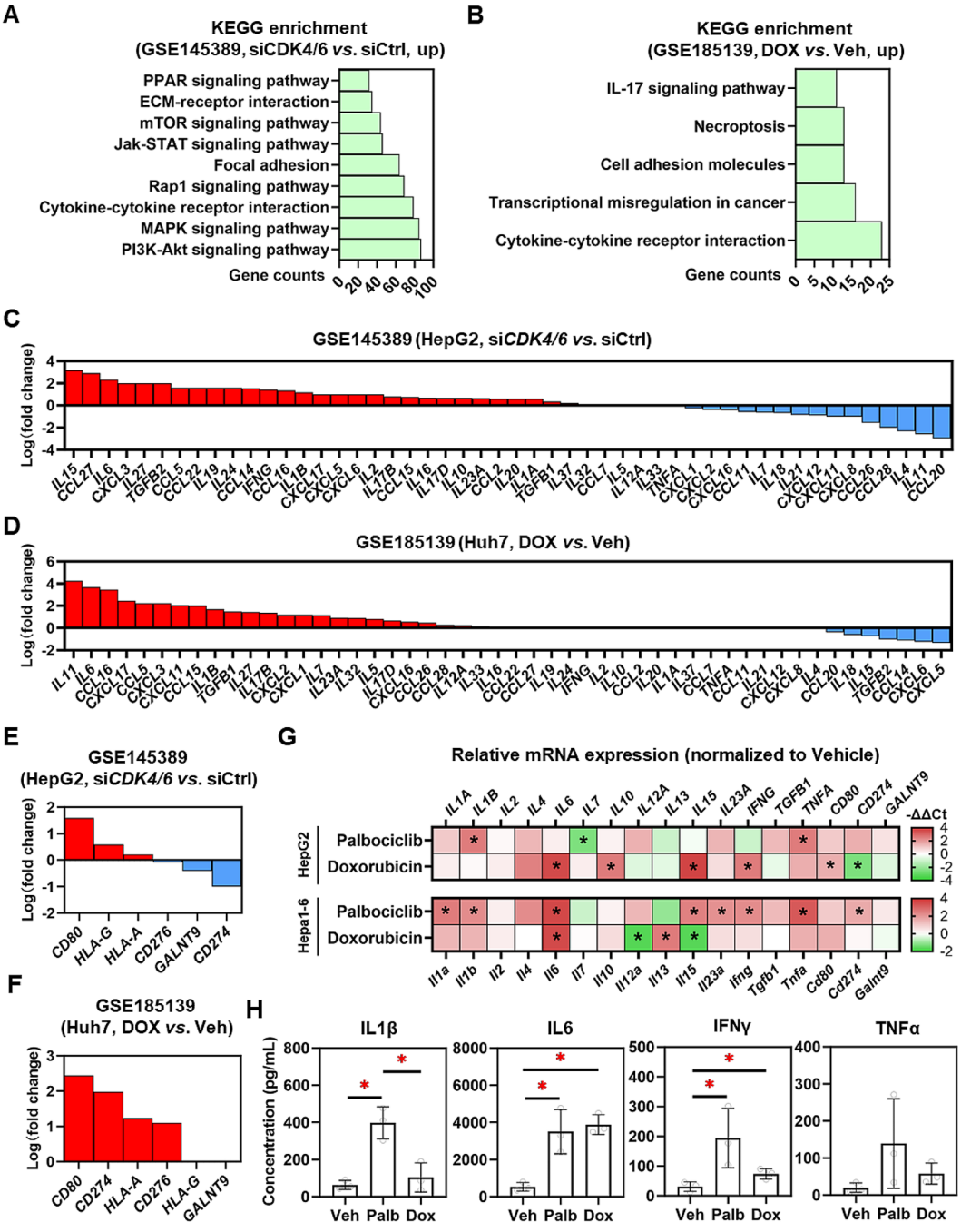

Fig. 4 CDK4/6 inhibition alters transcriptome and secretome of HCC cells. (**A**) KEGG enrichment was displayed based on significantly upregulated genes based on Palbociclib- (**A**) and Doxorubicin-treated (**B**) HCC cells (Treated vs. Vehicle). Fold changes of common inflammatory cytokines were displayed based on Palbociclib- (**C**) and Doxorubicin-treated (**D**) HCC cells (Treated vs. Vehicle). Fold changes of common immune checkpoints were displayed based on Palbociclib- (**E**) and Doxorubicin-treated (**F**) HCC cells (Treated vs. Vehicle). (**G**) Gene expression of common inflammatory markers and immune checkpoints measured in HepG2 and Hepa1-6 cells. (**H**) Concentrations of IL1β, IL6, IFNγ and TNFα measured by ELISA. Abbreviation: Veh: Vehicle, Palb: Palbociclib, Dox: Doxorubicin. "*" represents $p < 0.05$

or Dox-CM (Fig. 5D). Simultaneously, the proportion of $PD1^+$ $CD4^+$ cells increased significantly in T cells treated with Palb-CM compared to both vehicle-CM-treated and the positive control T cells. (Fig. 5E). The proportions of $PD1^+$ $CD8^+$ cells increased significantly in all CM-treated T cells compared to the positive control T cells. Specifically, Palb-CM significantly increased the proportion of $PD1^+$ $CD8^+$ T cells in contrast to vehicle CM (Fig. 5F). Intracellular calcium activity assays indicated that both calcium intake and Calmodulin-1/2/3 protein levels were

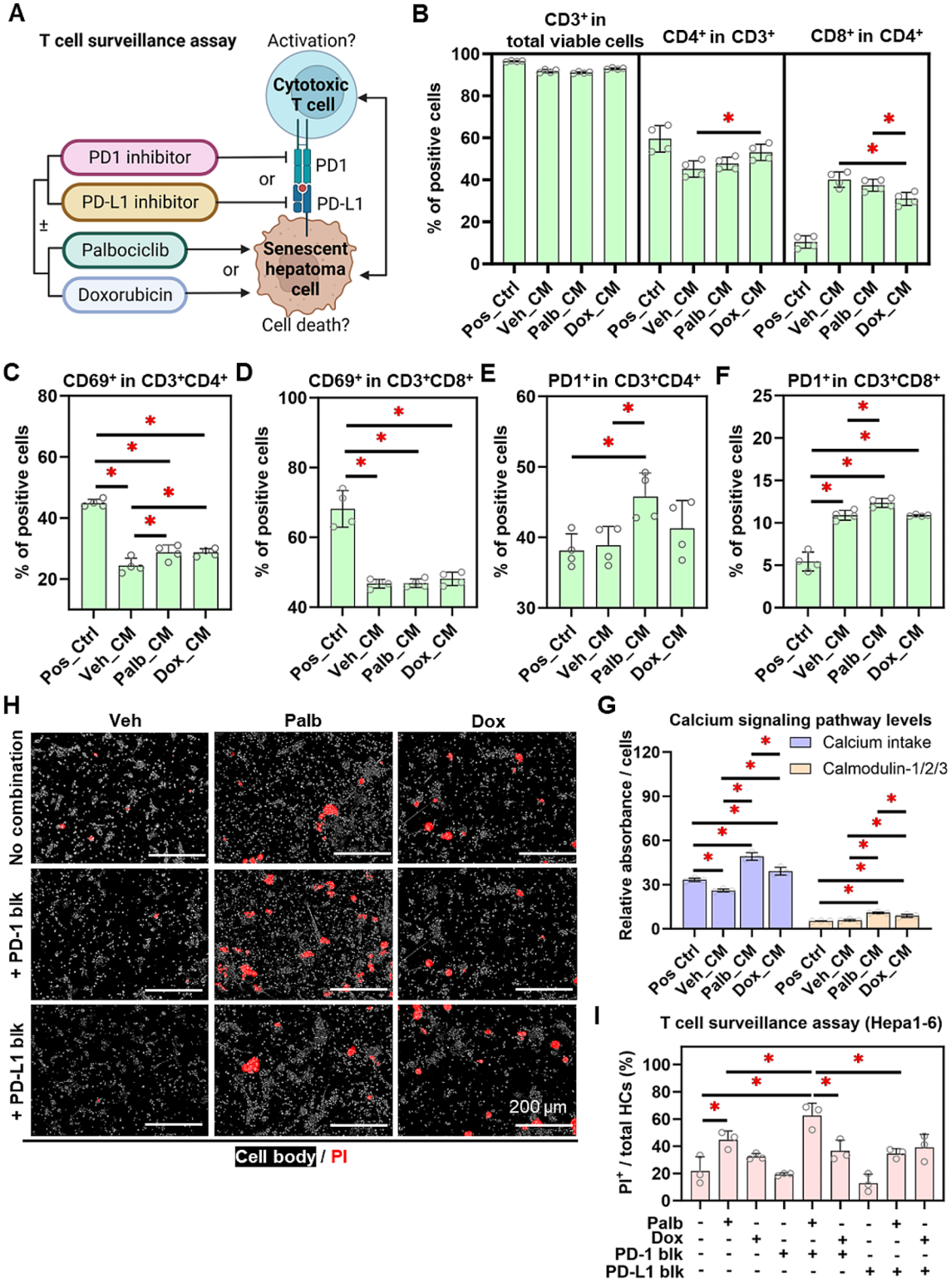

Fig. 5 T-cell surveillance altered by Palbociclib- and Doxorubicin-administrated HCC cells in combination with PD-1 or PD-L1 blockade. (**A**) T-cell surveillance assay strategy was schemed. (**B**) Under CM treatment and positive control administration, $CD3^+$ cells in total viable cells, $CD4^+$ cells in $CD3^+$ cells, and $CD8^+$ cells in $CD3^+$ cells. Flow cytometry determined the proportion of (**C**) $CD69^+$ cells in $CD3^+$ $CD4^+$ cells, (**D**) $CD69^+$ cells in $CD3^+$ $CD8^+$ cells, (**E**) $PD1^+$ cells in $CD3^+$ $CD4^+$ cells and (**F**) $PD1^+$ cells in $CD3^+$ $CD8^+$ cells. (**G**) Calcium intake and Calmodulin-1/2/3 levels on T cells were illustrated under CM treatment and positive control administration. (**H**) Co-cultivated with T cells, HC death was detected (PI^+) under the administration of Palbociclib, Doxorubicin, PD-1 inhibitor or PD-L1 inhibitor. (**I**) Dead cell proportion was evaluated. Abbreviation: Veh: Vehicle, Palb: Palbociclib, Dox: Doxorubicin, Ctrl: Control, CM: conditioned medium, blk: blockade. "*" represents $p < 0.05$

elevated by Palb-CM compared to vehicle CM, with the extent of this elevation even higher than that observed with Dox-CM, which evidenced active status of T cells (Fig. 5G). At the experiment endpoint, PD-1 and -L1 blockade didn't alter the T-cell-mediated cytotoxicity against untreated/proliferating HCs. Intriguingly, PD-1 blockade dramatically enhanced T-cell-mediated cytotoxicity against the Palb-induced senescent HCs, whereas PD-L1 blockade exhibited a limited T-cell derepressing effect in killing senescent HCs. In contrast, neither PD-1 nor PD-L1 blockade altered T-cell-mediated cytotoxicity against Dox-induced senescent HCC cells (Fig. 5H and I). Taken together, CDK4/6 inhibition-dependent senescence on HCC cells activates T cells and prevents cytotoxic T cells from PD-1/PD-L1-mediated exhaustion.

Discussions

Despite various novel treatment modalities for HCC management, the prognosis of HCC patients is still poor. Less than 20% of HCC patients are eligible for surgical tumor removal, urging the development of efficient therapies, especially for advanced HCC. Practically, systemic chemotherapies (e.g., Doxorubicin) serve as indispensable therapies for HCC patients though, concern was arisen about uninspiring outcome improvement and serious toxic side effects [24]. Trans-arterial chemoembolization and oral administration of targeted drugs (e.g., sorafenib) are currently most suggested in the clinical management of late-stage HCC patients [26]. However, above two-thirds of HCC patients could not benefit from these treatments, notably followed by acquired drug resistance. The immune modulation process is regarded as a promising approach to enhance precisive attacks on cancer cells, which may be blunted by the suppressive microenvironment blocking the activation and function of cytotoxic immune cells in most solid tumors, including HCC. Therefore, singular immune-enhancing or immune checkpoint-blocking therapy exerts negligible efficacy on HCC [27, 28].

T-cell surveillance is initially known as the framework to restrain chronic viral infection and pathogenic invasion [29]. Tumor-specific or tumor-associated antigen-presenting processes occur in almost all cancer cells, to attract both helper and cytotoxic T cells. However, established cancer entities cannot be easily eliminated by autologous T cells in vivo. This is partially attributed to T-cell exhaustion, which can be induced by PD-L1 binding to PD-1 molecules on activated T cells [30]. Later, with the discovery of various immune checkpoint proteins, PD-L1/PD-1 blockade gained a big victory in treating non-solid tumors, but it has posed a formidable challenge in the context of solid tumors [31]. Accordingly, it offers a promising prospect to improve the efficacy of immune checkpoint blockade in combination with chemotherapies or targeted therapies. Nevertheless, the high utility of adjuvant immuno-chemotherapy/targeted therapy remains challenging to acquire [32]. In recent decades, emerging studies have evidenced that tumor cells exert the potential to rewire the suppressive tumor microenvironment. Inimitably, cellular senescence may play a crucial role in fueling tumor progression and influencing immune surveillance [33]. The abundance and composition of SASPs vary from senescence-inducing approaches, exerting different regulatory effects on cancer cell immunogenicity and T-cell surveillance [34].

In this study, we characterized liver cancers from novel angles by conducting high-throughput transcriptome analysis on multiple HCC patient cohorts, identifying that cell-cycle regulators CDK4 and CDK6 significantly influence patients' outcomes. Interestingly, suppression of CDK4/6 may not only provoke inflammatory secretion of HCC cells but also improve $CD8^+$ T-cell-associated survival time. We also mined out elevated interactions between T cells and $CDK4/6^{low}$ HCC cells from single-cell RNA-seq datasets. Furthermore, we hypothesized that CDK4/6 suppression exaggerated the immunogenicity of HCC cells by the induction of cell-cycle arrest-dependent senescence. Doxorubicin (a DNA damage inducer) was introduced on HCC cells to compare with Palbociclib (a selective CDK4/6 inhibitor). Both two drugs appeared to induce HC senescence and strengthen immune factor expression. Nonetheless, they upregulated PD-L1 expression on HCs. Intriguingly, Palbociclib-induced senescent HCC cells promoted functional T-cell activation as evidenced by PD-1 upregulation. To dissect the contradictory results, T-cell cytotoxicity assays were performed to assess the actual cancer cell killing effects of T cells under either Palbociclib or Doxorubicin pre-treatments, along with either PD-1 or PD-L1 inhibitor. Results indicated that both drugs could promote the T-cell-mediated killing efficacy to a certain extent though, only the presence of PD-1 blockade further improves the T-cell cytotoxicity. Promisingly, we evidenced that CDK4/6 inhibition can not only depress HC proliferation but also lead to cytotoxic T-cell activation via senescence induction in HCs. Superior to DNA damage induction, CDK4/6 inhibition drastically promotes tumor immunogenicity. Our study certainly reveals a novel mechanism of CDK4/6 inhibition in treating HCC. What's more, the immunogenicity-enhancing effect of CDK4/6 inhibition antagonizes senescence-related T-cell exhaustion, which implies promising therapeutic strategies to combine CDK4/6 inhibitors with immune checkpoint blockades for HCC.

Hence, the lack of in-vivo HCC models in this study unfortunately weakened the mechanistic exploration. Initially, we anticipated establishing a primary HCC mouse model with carbon tetrachloride (CCL_4) administration

or a syngeneic mouse model transplanted with a highly proliferative HC line to investigate therapeutic efficacy and immune infiltration in vivo. Regrettably, CCL_4–induced tumor lesions exhibited heterogeneous CDK4/6 expression, while transplanted HCC cells failed to form convincing tumor lesions with typical tumor microenvironment. Thus, neither Palbociclib nor Doxorubicin treatments could be effectively resumed on these models. Hopefully, this issue may be resolved using our tailored in-vitro Liver-on-a-chip model currently under development, which harbors multiple cell types with dynamic immune cell circulation to recapitulate the tumor microenvironment [35]. Notably, cell-cycle regulation may act as a key metronome in reshaping tumor cell immunogenicity and modulating tumor immunity. For future perspectives, cellular senescence and SASPs appear to be promising therapeutic targets to protect against cancer.

Supplementary Information

The online version contains supplementary material available at https://doi.org/10.1186/s12935-024-03351-z.

Supplementary Material 1

Supplementary Material 2

Supplementary Material 3

Supplementary Material 4

Supplementary Material 5

Acknowledgements
We acknowledge support from Charité – Universitätsmedizin Berlin and Nanjing Medical University. Schematic figures were created via BioRender.

Author contributions
XC and HL conceived the topic. FT and AG advised the study. GY and HL performed bioinformatic analysis. XC, SC and HL performed biological experiments. HL drafted the manuscript and prepared the figures. XC, GY, and HL revised the manuscript. All authors have approved the published version of the manuscript.

Funding
Open Access funding enabled and organized by Projekt DEAL. This work was funded by National Nature Science Foundation of China (82300730), Changzhou (China) Health Commission (CZQM2022007 and QN202121), Changzhou (China) Science and Technology Bureau (CJ20220142), Changzhou Medical Center of Nanjing Medical University (CZKYCMCB202221) and German Research Foundation (DFG Ta434/8 – 1, SFB/TRR 296 and CRC1382, Project-ID 403224013). Xiurong Cai, Guo Yin and Hanyang Liu were funded by China Scholarship Council.

Data availability
Transcriptome data in this study are available from the GEO database. Other data presented in this study are available on request from the corresponding author.

Declarations

Ethics approval and consent to participate
Animal experiments in this study were approved by the Animal Welfare Committee of the affiliated Changzhou Second People's Hospital of Nanjing Medical University [Approval No. (2020) KYO 045 – 05].

Consent for publication
All authors have consented to the submission of this research paper.

Competing interests
Frank Tacke's lab has received research funding from Allergan, Bristol-Myers Squibb, Gilead and Inventiva. FT has received honoraria for consulting or lectures from Astra Zeneca, Gilead, AbbVie, BMS, Boehringer, Madrigal, Intercept, Falk, Ionis, Inventiva, Merz, Pfizer, Alnylam, NGM, CSL Behring, Novo Nordisk, Novartis.

Author details
[1]Department of Hematology, Oncology and Tumor Immunology, Charité Universitätsmedizin Berlin, Campus Virchow-Klinikum, 13353 Berlin, Germany
[2]The Jackson Laboratory, Bar Harbor, ME 04609, USA
[3]Department of Hepatology and Gastroenterology, Charité Universitätsmedizin Berlin, Campus Virchow- Klinikum and Campus Charité Mitte, Augustenburger Platz. 1„ 13353 Berlin, Germany
[4]Department of General Surgery, Changzhou Medical Center, The Affiliated Changzhou Second People's Hospital of Nanjing Medical University, Nanjing Medical University, Changzhou 213000, China

Received: 3 November 2023 / Accepted: 30 April 2024
Published online: 20 June 2024

References

1. Llovet JM, Kelley RK, Villanueva A, Singal AG, Pikarsky E, Roayaie S, Lencioni R, Koike K, Zucman-Rossi J, Finn RS. Hepatocellular carcinoma. Nat Rev Dis Primers. 2021;7(1):6.
2. Forner A, Reig M, Bruix J. Hepatocellular carcinoma. Lancet. 2018;391(10127):1301–14.
3. Llovet JM, Pinyol R, Kelley RK, El-Khoueiry A, Reeves HL, Wang XW, Gores GJ, Villanueva A. Molecular pathogenesis and systemic therapies for hepatocellular carcinoma. Nat Cancer. 2022;3(4):386–401.
4. Donisi C, Puzzoni M, Ziranu P, Lai E, Mariani S, Saba G, Impera V, Dubois M, Persano M, Migliari M, et al. Immune checkpoint inhibitors in the treatment of HCC. Front Oncol. 2020;10:601240.
5. Huang Y, Wu H, Li X. Novel sequential treatment with palbociclib enhances the effect of cisplatin in RB-proficient triple-negative breast cancer. Cancer Cell Int. 20;501:(2020). https://doi.org/10.1186/s12935-020-01597-x.
6. O'Leary B, Finn RS, Turner NC. Treating cancer with selective CDK4/6 inhibitors. Nat Rev Clin Oncol. 2016;13(7):417–30.
7. Hsu SK, Li CY, Lin IL, Syue WJ, Chen YF, Cheng KC, Teng YN, Lin YH, Yen CH, Chiu CC. Inflammation-related pyroptosis, a novel programmed cell death pathway, and its crosstalk with immune therapy in cancer treatment. Theranostics. 2021;11(18):8813–35.
8. Chen HA, Ho YJ, Mezzadra R, Adrover JM, Smolkin R, Zhu C, Woess K, Bernstein N, Schmitt G, Fong L, et al. Senescence Rewires Microenvironment sensing to facilitate Antitumor Immunity. Cancer Discov. 2023;13(2):432–53.
9. Marin I, Boix O, Garcia-Garijo A, Sirois I, Caballe A, Zarzuela E, Ruano I, Attolini CS, Prats N, Lopez-Dominguez JA, et al. Cellular Senescence is immunogenic and promotes Antitumor Immunity. Cancer Discov. 2023;13(2):410–31.
10. Lan C, Kitano Y, Yamashita YI, Yamao T, Kajiyama K, Yoshizumi T, Fukuzawa K, Sugimachi K, Ikeda Y, Takamori H, et al. Cancer-associated fibroblast senescence and its relation with tumour-infiltrating lymphocytes and PD-L1 expressions in intrahepatic cholangiocarcinoma. Br J Cancer. 2022;126(2):219–27.
11. Wang TW, Johmura Y, Suzuki N, Omori S, Migita T, Yamaguchi K, Hatakeyama S, Yamazaki S, Shimizu E, Imoto S, et al. Blocking PD-L1-PD-1 improves senescence surveillance and ageing phenotypes. Nature. 2022;611(7935):358–64.
12. Reimann M, Schrezenmeier J, Richter-Pechanska P, Dolnik A, Hick TP, Schleich K, Cai X, Fan DNY, Lohneis P, Masswig S, et al. Adaptive T-cell immunity controls senescence-prone MyD88- or CARD11-mutant B-cell lymphomas. Blood. 2021;137(20):2785–99.
13. Ritchie ME, Phipson B, Wu D, Hu Y, Law CW, Shi W, Smyth GK. Limma powers differential expression analyses for RNA-sequencing and microarray studies. Nucleic Acids Res. 2015;43(7):e47.
14. Li C, Tang Z, Zhang W, Ye Z, Liu F. GEPIA2021: integrating multiple deconvolution-based analysis into GEPIA. Nucleic Acids Res. 2021;49(W1):W242–6.

15. Blum A, Wang P, Zenklusen JC. SnapShot: TCGA-Analyzed tumors. Cell. 2018;173(2):530.
16. Consortium GT. The genotype-tissue expression (GTEx) project. Nat Genet. 2013;45(6):580–5.
17. Gu Z, Hubschmann D. Make interactive Complex heatmaps in R. Bioinformatics. 2022;38(5):1460–2.
18. Gene Ontology C. Gene Ontology Consortium: going forward. Nucleic Acids Res. 2015;43(Database issue):D1049–1056.
19. Kanehisa M, Furumichi M, Tanabe M, Sato Y, Morishima K. KEGG: new perspectives on genomes, pathways, diseases and drugs. Nucleic Acids Res. 2017;45(D1):D353–61.
20. Li T, Fan J, Wang B, Traugh N, Chen Q, Liu JS, Li B, Liu XS. TIMER: a web server for Comprehensive Analysis of Tumor-infiltrating Immune cells. Cancer Res. 2017;77(21):e108–10.
21. Newman AM, Liu CL, Green MR, Gentles AJ, Feng W, Xu Y, Hoang CD, Diehn M, Alizadeh AA. Robust enumeration of cell subsets from tissue expression profiles. Nat Methods. 2015;12(5):453–7.
22. Butler A, Hoffman P, Smibert P, Papalexi E, Satija R. Integrating single-cell transcriptomic data across different conditions, technologies, and species. Nat Biotechnol. 2018;36(5):411–20.
23. Jin S, Guerrero-Juarez CF, Zhang L, Chang I, Ramos R, Kuan CH, Myung P, Plikus MV, Nie Q. Inference and analysis of cell-cell communication using CellChat. Nat Commun. 2021;12(1):1088.
24. Gustavsson EK, Zhang D, Reynolds RH, Garcia-Ruiz S, Ryten M. Ggtranscript: an R package for the visualization and interpretation of transcript isoforms using ggplot2. Bioinformatics. 2022;38(15):3844–6.
25. Yang C, Zhang H, Zhang L, Zhu AX, Bernards R, Qin W, Wang C. Evolving therapeutic landscape of advanced hepatocellular carcinoma. Nat Rev Gastroenterol Hepatol. 2023;20(4):203–22.
26. Tang W, Chen Z, Zhang W, Cheng Y, Zhang B, Wu F, Wang Q, Wang S, Rong D, Reiter FP, et al. The mechanisms of sorafenib resistance in hepatocellular carcinoma: theoretical basis and therapeutic aspects. Signal Transduct Target Ther. 2020;5(1):87.
27. Brouillet A, Lafdil F. Risk factors of primary liver cancer initiation associated with tumour initiating cell emergence: novel targets for promising preventive therapies. eGastroenterology. 2023;1:e100010. https://doi.org/10.1136/egastro-2023-100010.
28. Llovet JM, Castet F, Heikenwalder M, Maini MK, Mazzaferro V, Pinato DJ, Pikarsky E, Zhu AX, Finn RS. Immunotherapies for hepatocellular carcinoma. Nat Rev Clin Oncol. 2022;19(3):151–72.
29. Blank CU, Haining WN, Held W, Hogan PG, Kallies A, Lugli E, Lynn RC, Philip M, Rao A, Restifo NP, et al. Defining 'T cell exhaustion'. Nat Rev Immunol. 2019;19(11):665–74.
30. Belk JA, Daniel B, Satpathy AT. Epigenetic regulation of T cell exhaustion. Nat Immunol. 2022;23(6):848–60.
31. Makuku R, Khalili N, Razi S, Keshavarz-Fathi M, Rezaei N. Current and Future Perspectives of PD-1/PDL-1 Blockade in Cancer Immunotherapy. *J Immunol Res* 2021, 2021:6661406.
32. Ghahremanloo A, Soltani A, Modaresi SMS, Hashemy SI. Recent advances in the clinical development of immune checkpoint blockade therapy. Cell Oncol (Dordr). 2019;42(5):609–26.
33. Schmitt CA, Wang B, Demaria M. Senescence and cancer - role and therapeutic opportunities. Nat Rev Clin Oncol. 2022;19(10):619–36.
34. Cai X, Guillot A, Liu H. Cellular Senescence in Hepatocellular Carcinoma: the passenger or the driver? *Cells* 2022, 12(1).
35. Liu H, Kohlhepp M, Yin G, Hundertmark J, Heymann F, Aina K, Mosig A, Tacke F, Guillot A. Dissecting NAFLD pathomechanisms using primary mouse liver and blood cells in a microfluidic perfusable compartmentalized liver-on-a-chip model. J Hepatol. 2023;78:S87.

Publisher's Note